The Company of **Biologists**

RESEARCH ARTICLE

Hyperbaric tracheobronchial compression in cetaceans and pinnipeds

Michael Denk[1],*, Andreas Fahlman[2], Sophie Dennison-Gibby[3], Zhongchang Song[4,5] and Michael Moore[4]

ABSTRACT

Assessment of the compressibility of marine mammal airways at depth is crucial to understanding vital physiological processes such as gas exchange during diving. Very few studies have directly assessed changes in cetacean and pinniped tracheobronchial shape, and none have quantified changes in volume with increasing pressure. A harbor seal, gray seal, harp seal, harbor porpoise and common dolphin were imaged promptly post mortem via computed tomography in a radiolucent hyperbaric chamber. Volume reconstructions were performed of segments of the trachea and bronchi of the pinnipeds and bronchi of the cetaceans for each pressure treatment. All specimens examined demonstrated significant decreases in airway volume with increasing pressure, with those of the harbor seal and common dolphin nearing complete collapse at the highest pressures. The common dolphin bronchi demonstrated distinctly different compression dynamics between 50% and 100% lung inflation treatments, indicating the importance of air in maintaining patent airways, and collapse occurred caudally to cranially in the 50% treatment. Dynamics of the harbor seal and gray seal airways indicated that the trachea was less compliant than the bronchi. These findings indicate potential species-specific variability in airway compliance, and cessation of gas exchange may occur at greater depths than those predicted in models assuming rigid airways. This may potentially increase the likelihood of decompression sickness in these animals during diving.

KEY WORDS: Computed tomography, Marine mammal, Trachea, Bronchi, Airway compression

INTRODUCTION

Diving marine mammals face numerous environmental challenges, including pressure gradients during diving. Rather than rigidly resist this pressure, the compliant ribcage structure of marine mammals has been shown to compress with increasing pressure at depth (Moore et al., 2011; Ridgway et al., 1969). How does the respiratory tract respond to this compression? Scholander (1940) proposed that alveoli collapse under pressure, channeling air from the alveolar gas exchange surfaces to the more rigid upper airway structures such as

[1]Kansas State University College of Veterinary Medicine, Manhattan, KS 66502, USA. [2]Fundación Oceanogràfic de la Comunitat Valenciana, Gran Vía Marqués del Turia 19, 46005 Valencia, Spain. [3]Televet Imaging Solutions, PLLC, Oakton, VA 22124, USA. [4]Biology Department, Woods Hole Oceanographic Institution, Woods Hole, MA 02543, USA. [5]Key Laboratory of Underwater Acoustic Communication and Marine Information Technology of the Ministry of Education, College of Ocean and Earth Sciences, Xiamen University, Xiamen 361005, People's Republic of China.

*Author for correspondence (m51988@ksu.edu)

ⓘ M.D., 0000-0001-9678-189X; A.F., 0000-0002-8675-6479; Z.S., 0000-0002-5259-5718

the trachea. Leith similarly suggested that the stiff cartilage-armored airways of marine mammals may function as air-filled 'reservoirs' by receiving alveolar gas from the lungs at depth (Leith, 1989; Leith et al., 1972). Compression of the lungs and alveolar collapse has been shown to result in a pulmonary shunt (Kooyman and Sinnett, 1982; McDonald and Ponganis, 2012), halting gas exchange and possibly reducing the likelihood of decompression sickness. This 'balloon-pipe' model has been used to model the theoretical depth at which the alveoli collapse and the pulmonary shunt occurs (Stephenson, 2005).

Alveolar compression and the depth at which gas exchange ceases in cetaceans and pinnipeds has been more directly inferred by a wide range of means, including blood and tissue N_2 and O_2 measurements (Kooyman et al., 1972; Kooyman and Sinnett, 1982; McDonald and Ponganis, 2012; Ridgway and Howard, 1979). Computed tomographic (CT) imaging of cetacean and pinniped cadavers in a hyperbaric chamber has visually demonstrated the voiding of air from the periphery of the lungs and their change in volume at simulated depths (Moore et al., 2011). Fewer studies have examined the degree of compression of the mainstem bronchi and trachea at depth. Kooyman et al. (1970) measured the 2D compression of the trachea and bronchi via radiograms in a northern elephant seal (*Mirounga angustirostris*) and a Weddell seal (*Leptonychotes weddellii*) maintained in pressure chambers. The trachea was found to compress to less than half of normal diameter in both animals within the dorsoventral plane at pressures of 31.6 atmosphere absolute (ata) (306 m), while the bronchi-bronchioles demonstrated no appreciable change in their diameter (Kooyman et al., 1970).
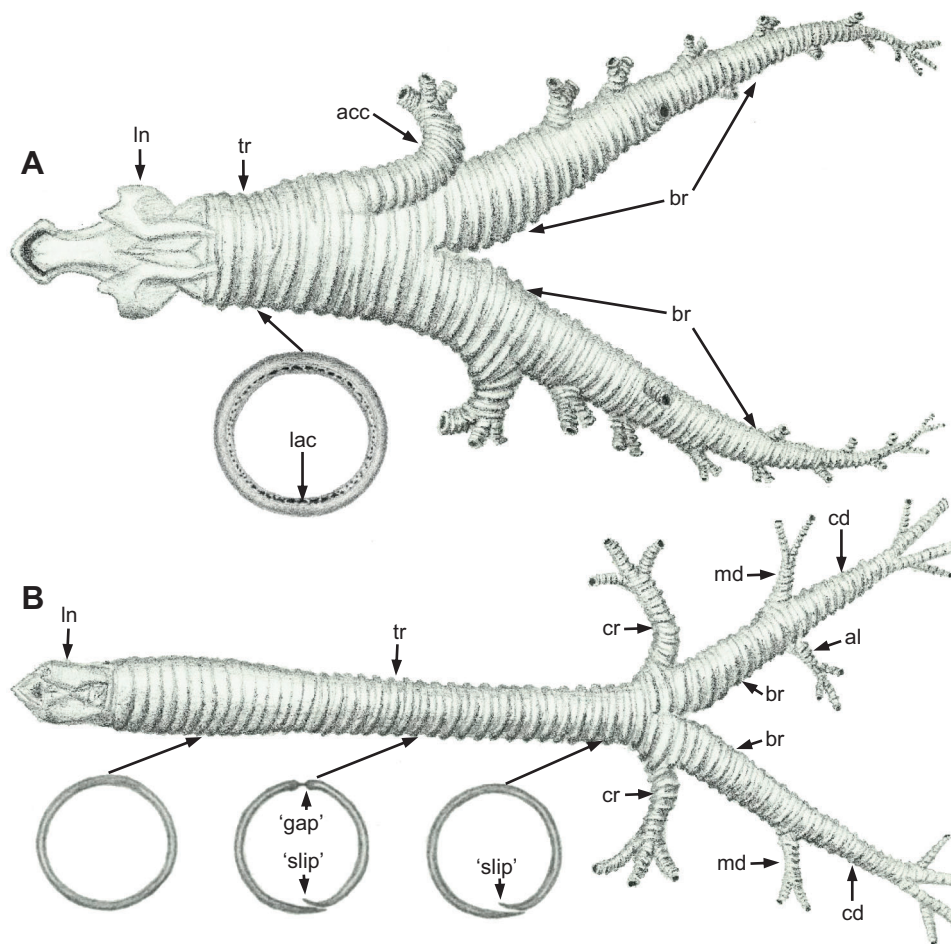
Anatomical study of the airways reveals a wide range of architectural elements suggestive of varying degrees of compressibility. The cetacean tracheobronchial tree is characterized by a very short, wide trachea featuring extensive venous vasculature within the submucosa (vascular lacunae), and continuous spiraling tracheal rings (Fig. 1A) (Ballarin et al., 2018; Cozzi et al., 2005; Moore et al., 2014). Cetacean right and left lungs are unilobular; a prominent right tracheal bronchus branches into the right lung, and the two large tapering primary bronchi give rise to dorsal, lateral and medial branches along their length that further ramify into the lung tissue (Fig. 1A) (Kida, 1990; Nakakuki, 1994). In contrast, the pinniped tracheobronchial tree begins with a longer trachea lacking the lacunae and consisting of a variety of continuous and discontinuous tracheal ring configurations (Fig. 1B) (Kooyman and Andersen, 1969; Moore et al., 2014; Tarasoff and Kooyman, 1973). Pinniped lungs are divided into cranial, middle and caudal, and accessory lobes, and like many terrestrial animals the primary bronchi bifurcate into lobar branches corresponding to these divisions (Fig. 1B) (Laakkonen and Jernvall, 2016; Tarasoff and Kooyman, 1973).

Measuring the compliance of the conducting airways (trachea and bronchi) is important as this affects alveolar compression, the depth

Fig. 1. Illustrations of cetacean and pinniped tracheobronchial trees and tracheal cross-sections. (A) Common dolphin and (B) harbor seal. Note the differences in tracheal proportions and structure. The common dolphin features multiple small dorsal, lateral and medial branches of the mainstem bronchi serving the unilobular right and left lungs, while the harbor seal features lobar bronchial branching representative of the distinct lung lobes. acc, accessory bronchus; al, accessory lobar bronchus; br, main stem bronchus; cd, caudal lobar bronchus; cr, cranial lobar bronchus; lac, vascular lacunae; ln, larynx; md, middle lobar bronchus; tr, trachea. Illustrations drawn by M.D. from IFAW 10-065 Dd and DO 8811 computed tomography (CT) data.

of alveolar collapse, and gas exchange dynamics. If the trachea is compressible, models predict that the depth of alveolar collapse will be greater than if the trachea was a rigid pipe (Bostrom et al., 2008), which will have a major effect on blood and tissue gas tensions (Fahlman et al., 2009, 2018; Hodanbosi et al., 2016). Increased gas exchange at depth may increase the N_2 blood and tissue tension, supersaturation and the likelihood of bubble formation during ascent (Hooker et al., 2009). Studies involving arterial O_2 measurements in sea lions indicate that gas exchange is still occurring at depths below which the alveoli have previously been estimated to collapse (McDonald and Ponganis, 2012; Tift et al., 2017). To improve our understanding of gas exchange, and the potential cardio-respiratory limitations while diving, there is therefore a need to more clearly establish the extent of tracheal and bronchial compression during thoracic compression at depth. The most direct methods to establish such potential changes are through cross-sectional imaging methods such as CT and magnetic resonance imaging. The primary objectives of this study were therefore to (1) identify via CT data whether there are volume

changes within the trachea and bronchi of five deceased marine mammal species under varying pressures, and (2) quantify these changes via CT volume rendering techniques for comparison across species.

MATERIALS AND METHODS
This study utilized CT data obtained from marine mammal cadavers in a radiolucent hyperbaric chamber as previously described in Moore et al. (2011). A gray seal [*Halichoerus grypus* (Fabricius)], harbor seal (*Phoca vitulina* Linnaeus) and harp seal (*Pagophilus groenlandicus* Erxleben), which were all drowned in fishing nets, as well as a harbor porpoise [*Phocoena phocoena* (Linnaeus)] and a common dolphin (*Delphinus delphis* Linnaeus) both found beached and freshly dead, were all transported to the laboratory. A summary of all animals and pressure treatments used in this study can be found in Table 1. Deceased animals were received under NOAA permit no. 932-1905-00/MA-009526 if fishery bycaught, and under a letter from the NOAA Greater Atlantic Regional Fisheries Office to M.M. if stranded. Ambient mean temperatures during transport

Table 1. All specimens, air inflation treatments and depth treatments

Common name	ID	Sex	Length (cm)	Mass (kg)	Source	Lung inflation treatments (ml)	Depth treatments (m)
Harp seal	DO 5952	F	99	27.5	Bycaught	1200 (full)	0, 49.6, 93.7
Harbor seal	DO 8811	F	104	25.6	Bycaught	600 (half)	0, 49.6, 97.8
Gray seal	DO 8883	F	104	21.35	Bycaught	600 (half)	0, 24.8, 49.6
Harbor porpoise	IFAW 10–049 Pp	M	105	22.1	Single stranded	1800 (full), 900 (half)	0, 49.6, 97.84/95.77
Short-beaked common dolphin	IFAW 10–065 Dd	M	130	75.03	Mass stranded	3000 (full), 1500 (half)	0, 49.6, 93.7

to the laboratory ranged from −3 to 1°C, and transport time did not exceed 24 h. Upon arrival, the specimens were stored at 4°C until each experiment began, less than 12 h after arrival at the laboratory. No specimens were frozen. The trachea of each animal was intubated with the endo-tracheal tube (ET) attached to a system of 3-way valves. A 3 l volumetric syringe (Series 5530, Hans-Rudolph Inc., Shawnee, KS, USA) was connected to the valves, which allowed inflation of the lungs at increments of 100 ml (see Moore et al., 2011, for further details).

The total lung capacity (TLC) was evaluated for each specimen by inflating the lungs of the intact specimen to a trans-thoracic pressure (P_{tp}=P_{air}−P_{lung}) of 30 cmH$_2$O (Fahlman et al., 2011; Kooyman and Sinnett, 1982). This non-standard estimate of TLC includes the compliance of both the lung and the thorax; we also determined the more standard estimate of TLC based on lungs excised from the thoracic cavity. To separate the two, we call the former TLC$_{tt}$, and the latter TLC$_{ex}$, for trans-thoracic total lung capacity and excised total lung capacity, respectively (see Table 2 for a summary of these values and percentage change between them for each animal). Hyperbaric experiments were subsequently performed by inflating the lungs to 50% or 100% of TLC$_{tt}$. For each experiment, the specimen was placed in sternal recumbency in the imaging portion of the chamber. To secure the specimen in the chamber for avoidance of specimen rotation and position changes as buoyancy decreased with depth, suction cups were attached to the ventrum in multiple places and the cups pressed on to the chamber wall. The chamber was filled with water and all animals except for the gray seal were pressurized to ca. 11 ata (1 ata=98.1 kPa=14.2 psi) and 6 ata, representing simulated diving depths of ca. 100 m and 50 m, respectively. The gray seal was pressurized to 6 ata and 3.5 ata, simulating diving depths of circa 50 m and 25 m, respectively. Scans were made at each of two pressures and also at 1 ata (0 psi), which represented the surface. After each experiment was concluded, gross necropsy and histological examinations were undertaken.

The current study utilized a subset of relative inflation volumes for the cetaceans (50% and 100% of TLC$_{tt}$), harp seal (100% of TLC$_{tt}$), and gray and harbor seals (50% of TLC$_{tt}$). The remaining scans were not utilized as body fluids within the airways obscured their borders. A Somatom Volume Zoom 4-detector row multi-slice scanner (Siemens Medical Solutions USA Inc., Malvern, PA, USA) was used for all image acquisitions. All scans were performed using a high exposure helical scan protocol of 800 (effective) mA and 140 kV with a 0.5 s rotation time with 6 mm thick slices, using a 5 mm collimator and a table pitch of 10 mm. Two sets of reconstructions for each pressure were done at 6 mm intervals using B30 (soft tissue) and B70 (bone/lung) algorithms. Following each pressurization, the chamber was removed from the scanner bed, drained and the end cap removed to gain access to the endotracheal tube valve to adjust the lung inflation volume.

Table 2. Comparison of TLC$_{ex}$ and TLC$_{tt}$ values for all specimens with calculated percentage change

| Common name	TLC$_{ex}$ (ml)	TLC$_{tt}$ (ml)	% Change
Harp seal	2848	1200	57.9
Harbor seal	2666	1200	55
Gray seal	2261	1200	46.9
Harbor porpoise	2329	1800	22.7
Short-beaked common dolphin	7168	3000	58.1

TLC$_{ex}$ is defined by the following formula as derived via excised lung studies (Kooyman,1973; Fahlman et al., 2011): 0.135×(animal mass in kg$^{0.92}$). TLC$_{tt}$ is defined as inflating the lungs of an intact cadaver to a trans-thoracic pressure (P_{tp}=P_{air}−P_{lung}) of 30 cmH$_2$O.

OsiriX Lite software was utilized to manually segment the lumen of bronchial and tracheal sections on each scan slice, after which a volume rendering was performed to calculate the luminal volume measurement. Prior to segmentation, the viewing window was adjusted to allow reliable airway visualization for all animals throughout every pressure treatment (window level, WL: −148; window width, WW: 1638; magnification 350×). All airway luminal measurement borders were defined by the transition from gas attenuation Hounsfield unit values to the soft tissue attenuation Hounsfield unit values of the airway wall (mucosa); only the gas components were segmented. Bronchial volumes were calculated separately for the left and right by means of pre-determined start and end points within the scans. Pre-processing evaluation of the scans revealed the tendency of the entire bronchial tree to travel cranially within the thoracic cavity under increasing pressure. As a result, bony landmarks such as vertebral or rib count could not be used for start and end points, as their relationships to the airways changed between pressure treatments. Therefore, the start and end points for segmentation and volume calculation were established by means of branching patterns within the airways themselves. Considering the differences in bronchial branching patterns between cetaceans and pinnipeds, an approach was taken to measure the majority of the large airway volume to provide functional units which could be compared between species. In cetaceans, bronchial volumes were measured from the tracheal bifurcation as a start point and through the entire length of the primary bronchus, ending at the terminal bifurcation of the primary bronchus as the end point. In pinnipeds, bronchial volumes were measured from the tracheal bifurcation as the start point to the end of the caudal secondary (lobar) bronchus as the end point. This provided reliable measurement of most of the large airway volume of the specimens.

Because of intubation of the relatively short cetacean trachea, tracheal measurements unaffected by the presence of the ET tube could not be achieved in the cetaceans. Pinniped tracheal measurements were obtained distal to the tip of the ET tube. Measurement of the seal tracheal volumes was complicated by the apparent presence of body fluids within the lumen of the trachea. Representative caudal segments that were not influenced by the fluid content in every pressure treatment for a given individual were identified and measured. All tracheal endpoints were determined by starting at the tracheal bifurcation and measuring cranially to an endpoint determined by a consistent number of CT slices established for all pressure treatments of a given animal. This segment represented the maximum amount of tracheal length, equal throughout all pressure treatments, that was unaffected by the ET tube or fluid infiltration in every treatment. In the harp, harbor and gray seals, these segments were 2, 4 and 15 slices long, respectively. Percentage change between volumes at the various pressures was calculated via the following formula: [(current volume−volume at 0 kPa)/volume at 0 kPa]×100. Therefore, the two figures obtained for the two pressurizations of a given treatment were calculated as negative percentage changes, both relative to the volume at the surface.

RESULTS

All tracheal and bronchial segments experienced decreases in luminal volume with increasing pressure (Figs 2 and 3). The common dolphin bronchi (full and half inflation treatments) and harbor seal trachea and bronchi (half inflation treatment) exhibited near-complete collapse at the highest simulated depth (common dolphin: Figs 4A and 5). The bronchi of the harbor porpoise and harp seal experienced significant decreases in volume, but remained
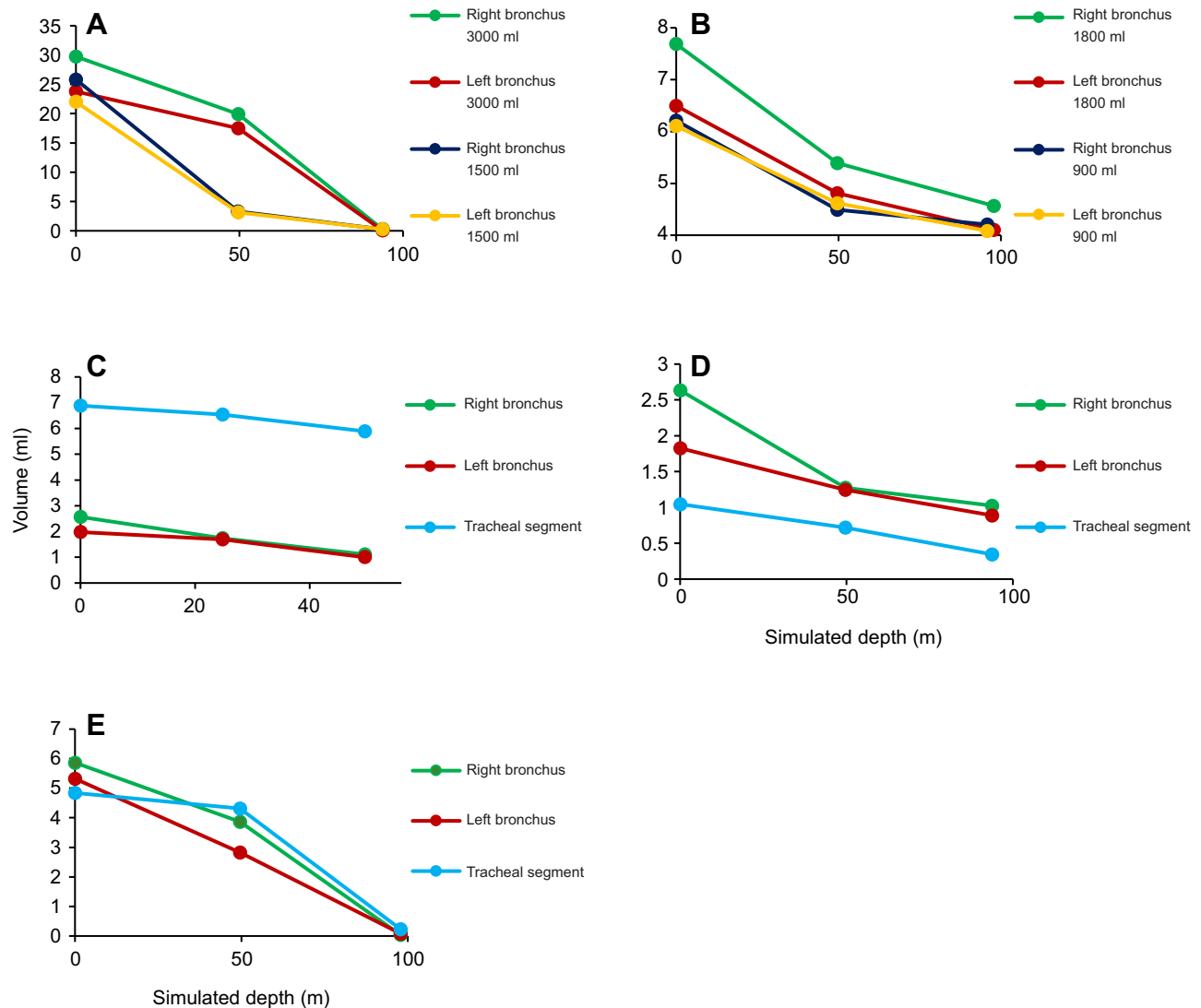
Fig. 2. Absolute airway volume plotted against simulated depth for all five specimens. (A) Common dolphin, (B) harbor porpoise, (C) gray seal, (D) harp seal and (E) harbor seal. Here, 1 m of simulated depth represents 0.1 kPa of pressure exerted on the specimen. Each specimen experienced the depth treatments once at each inflation treatment. Note the differential in compression dynamics between the 3000 ml and 1500 ml inflation treatments of the common dolphin.

open at all pressures tested (harp seal: Fig. 4B). The common dolphin displayed a differential in compression dynamics between the inflation treatments. When the lungs were inflated with 3000 ml of air (100% TLC_{tt}), the greatest percentage change in volume occurred between simulated depths of 50 and 100 m, while at the 1500 ml inflation (50% TLC_{tt}), the greatest percentage change occurred between the surface and 50 m (Fig. 3A). The harbor porpoise did not display these dynamics, showing the greatest percentage change between the surface and 50 m, regardless of the amount of air in the lungs (Fig. 3B). The gray and harbor seal tracheas demonstrated a comparatively smaller percentage change than the bronchi at depths from 0 to 50 m (Fig. 3C,E). The harp seal trachea, in contrast, demonstrated a steeply linear percentage decrease equivalent to that of the bronchi (Fig. 3D). Dorsoventral compression was evidenced by visual narrowing and flattening of the bronchial lumen. In the common dolphin half volume inflation treatment, this occurred in a caudal to cranial order (Fig. 5B). Craniocaudal compression was evidenced by a decrease in the number of slices needed to reach the previously determined

endpoints (Fig. 6). The decrease of the airway volume in these two planes was paralleled by compression of the lungs, the proportions of which also decreased in the ventrodorsal and craniocaudal directions (Fig. 6).

DISCUSSION
The airway dynamics observed in this study indicate that the trachea and bronchi do not behave as rigid pipe-like structures. Rather, they are flexible and compressible to varying degrees depending on the species and the simulated diving lung volume. Furthermore, airways in all animals examined demonstrated the ability to return to an open position after compression, regardless of maximum compression pressure or inflation treatment. These results stand in contrast to the historic assumptions of airway dynamics (Scholander, 1940), and support previous studies indicating compressible airways (Kooyman et al., 1970, 1999; Moore et al., 2014). This suggests that there may be significant differences in lung compression and pulmonary shunt between species, which will affect tissue and blood gas dynamics (Fahlman et al., 2009).
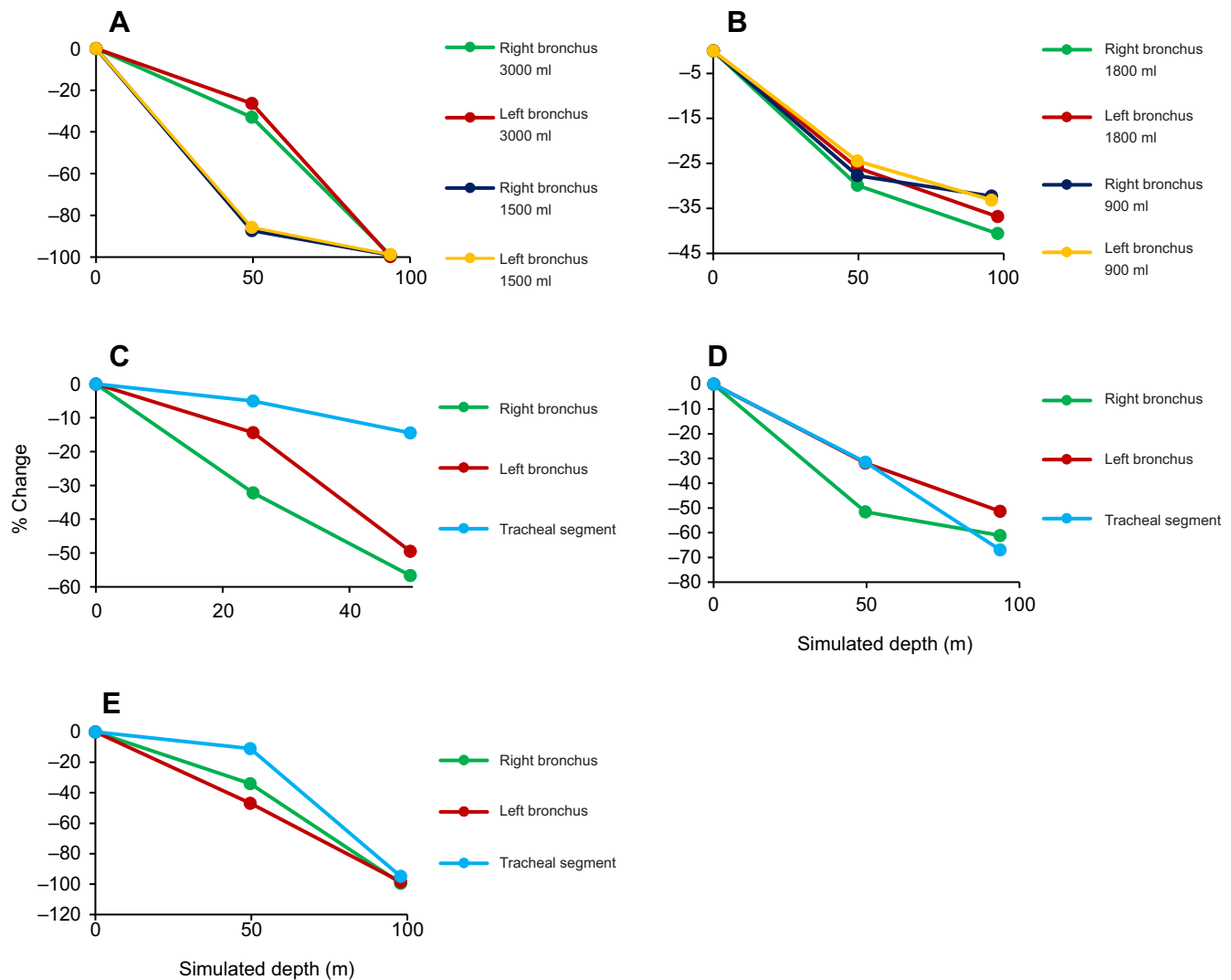
Fig. 3. Airway volume percentage change plotted against simulated depth for all five specimens. (A) Common dolphin, (B) harbor porpoise, (C) gray seal, (D) harp seal and (E) harbor seal. Here, 1 m of simulated depth represents 0.1 kPa of pressure exerted on the specimen. Each specimen experienced the depth treatments once at each inflation treatment. Note the differential in compression dynamics between the 3000 ml and 1500 ml inflation treatments of the common dolphin.

Prior to considering the possible physiological implications of these findings, it would be appropriate to discuss the relevant limitations in experimental technique and data processing. General differences between cetacean and pinniped airway proportions and air management must then be considered, to place the findings of this study in a taxa-relevant context. The airway compression results of the cetaceans and pinnipeds will then be analyzed separately. The unique physical properties and anatomy of the cetacean trachea will first be described to establish the context for the observed bronchial compression in the cetaceans. Comparison of bronchial collapse in the cetaceans within the context of inflation treatment and taxa-specific diving behavior will follow. Finally, a possible interpretation for the sequence of bronchial collapse for the common dolphin will be considered. As with the cetaceans, pinniped airway anatomy will then be discussed in the context of the dynamics of the tracheal and bronchial segments for each pinniped specimen, and functional significance will be proposed. Finally, some basic principles for future study of species-specific airway compression dynamics in pinnipeds will be suggested.

A limitation of this study was the 6 mm slice thickness of the scans, which did not correct for distortion due to obliquity in the volume measurements. As this obliquity remained consistent in the scans, however, any error present should also be consistent and should not affect the relative values of the measurements. We were also limited by the presence of body fluids in the tracheal lumen, which occurred in some specimens and for some lung inflations. This reduced the number of available treatments that could be used for this study as well as the ranges of the tracheal segments which could be measured. The ET intubation further limited the range of tracheal change that could be measured without interference.
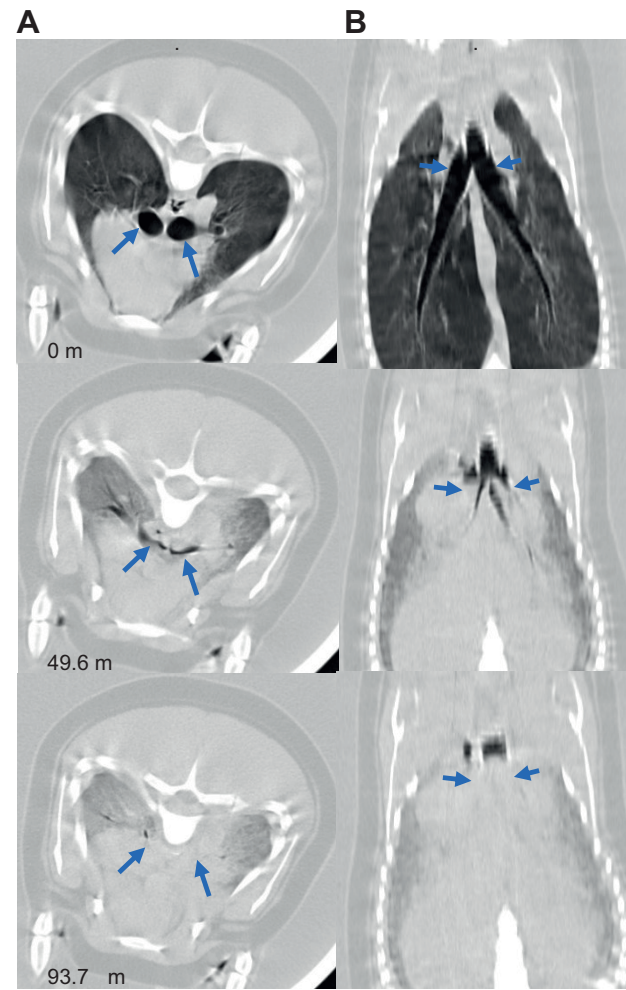
We also acknowledge the limitations of cadaver-based studies in inferring physiological principles. Most notable of these are the decreases in compliance related to rigor mortis events in postmortem tissues (Fitzgerald, 1975; Smith, 1939). While all specimens could be reliably determined to be code 2 (freshly dead), it is unlikely that the tissues had begun to decompose. Study of postmortem gross and histologic characteristics of bycaught versus stranded marine mammals indicates that acutely asphyxiated animals display no statistical increase in gas bubbles, congestion,
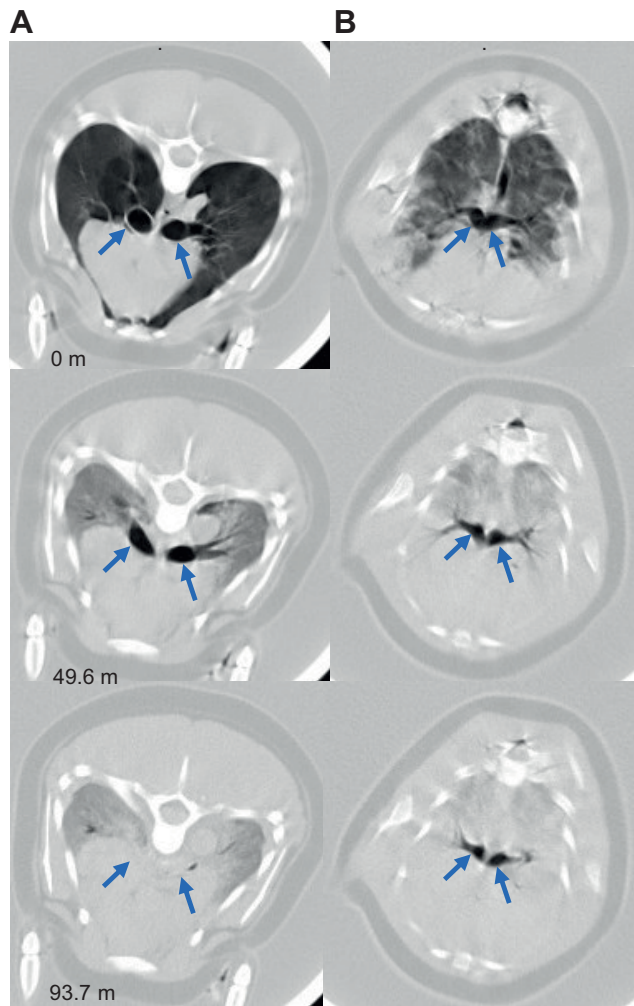
Fig. 4. Compression in tracheal bifurcations under pressure. (A) Common dolphin tracheal bifurcation (3000 ml of air in lungs, full lung volume treatment) demonstrating dorsoventral compression of the bronchi and with increasing simulated depth. (B) Harp seal tracheal bifurcation (1200 ml of air in lungs, full lung volume treatment), demonstrating mild compression but not complete collapse. Blue arrows indicate the location of the tracheal bifurcation; numbers indicate simulated depth in meters (m).

Fig. 5. Common dolphin tracheal bifurcation under pressure (1500 ml of air in lungs). (A) Axial and (B) 3D dorsal sections. Blue arrows mark the location of the tracheal bifurcation. Note the folding of the bronchi at the tracheal bifurcation in the 49.6 m treatment, as well as the caudal to cranial progression of collapse (B). Numbers indicate simulated depth in meters (m).

froth or fluid in the lungs/airways in comparison to non-drowned stranded animals (Bernaldo de Quirós et al., 2018).

TLC is usually estimated from excised tissues, but as we needed the carcasses intact for this study, we could not determine the TLC_{ex} before the experiment. We therefore estimated TLC_{tt}, or the pressure across the lung and the chest/thorax, which includes the compliance of both structures and results in a smaller TLC than that predicted from excised lungs. As a comparison, the lungs from all these specimens were later excised and the TLC_{ex} determined, which agreed well with the volume estimated from the equation: $TLC_{ex}=0.135×(mass\ in\ kg)^{0.92}$ (Table 2) (Fahlman et al., 2011; Kooyman, 1973). Thus, the TLC_{tt} measurements, with the exception of that for the harbor porpoise, are roughly half the volume of the predicted TLC_{ex}. The smaller measurements in the intact animals are due to the inward elastic recoil which resisted the outward expansion of the lungs during inflation. This restrictive effect could have varied in the cadavers as a result of different levels of rigor mortis affecting decreases in compliance of the thoracic cavity. The harbor porpoise showed the least percentage change between calculated and measured TLC, with a value of 22.7%

(Table 2); this specimen may have been more compliant as a consequence of a less advanced stage of the rigor mortis cycle in comparison to other specimens. In summary, the overall decreased compliance of the thoracic cavity in the cadavers may have resulted in underestimated TLC readings and consequently inflation treatments lower than the half and full TLC of a living animal. The smaller TLC measurements utilized for this study may therefore more correctly represent trans-thoracic pressures of 30 cmH_2O, rather than pure trans-pulmonary pressures of 30 cmH_2O, as a component of this pressure is due to the compliance of the thoracic cavity and not purely lung tissue. Alternatively, the predictions based upon excised lungs represent effects in structures inflated outside of their usual anatomical boundaries, which may result in larger TLC volumes than those of an intact animal. The statistical significance of pressure-related changes unfortunately could not be evaluated in this study because of the small sample size, which resulted from a limited availability of suitable specimens and scanner costs. Regardless of these limitations, this study provides an insight into the 3D structural characteristics of the air-filled airways under pressure *in situ*, which expands past 2D tracheal measurements (Kooyman et al., 1970), and studies of hyperbaric lung dynamics (Moore et al., 2014).
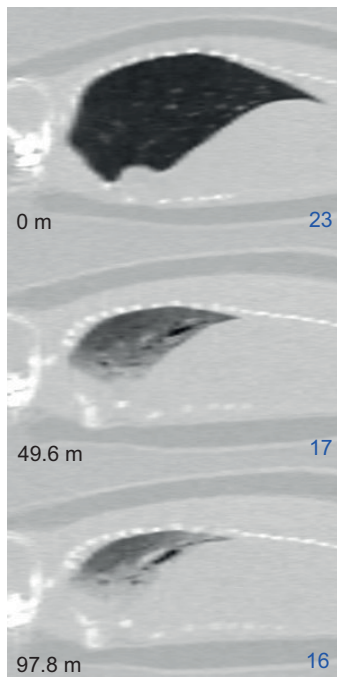
Fig. 6. Sagittal views of the harbor porpoise left lung lobe (1800 ml in lungs), illustrating craniocaudal as well as ventrodorsal compression. The blue values in the bottom right corners of each image are the total number of 6 mm CT slices needed to segment the bronchial volume within the pre-determined endpoints, indicating that the bronchi compress in the craniocaudal direction with the lungs. The black numbers indicate simulated depth in meters (m).

Both pinnipeds and cetaceans must solve the problems inherent in gas-filled airways during diving. While it was formerly believed that cetaceans dive with air-filled lungs whereas phocid pinnipeds dive after exhalation, it has been demonstrated that such reduction in diving lung volume in phocids represents only 20% of TLC (Falke et al., 2008). Species-specific differences in the morphology and geometry of cetacean and pinniped upper and lower airways may play a role in the importance of tracheal versus bronchial collapse and management of this air under pressure. In cetaceans, the trachea is broad but very short as a result of the truncated cervical structure, whereas the pinnipeds maintain a comparatively long cervical structure and tracheal length (Moore et al., 2014; Fig. 1). Therefore, in pinnipeds, the anatomical dead space of the trachea is proportionately larger than that of the main stem bronchi when compared with cetaceans. A pinniped may therefore benefit from a longer, potentially more rigid trachea receiving air from the collapsing bronchial structure. In the cetacean, however, collapsing bronchi would result in the rapid loss of the majority of anatomical dead space proximal to the larynx. This would initially appear to result in a more severe delay in voiding of air from the lungs in cetaceans as compared with pinnipeds. However, odontocete cetaceans produce sound within the upper respiratory tract by pneumatic means. During sound production in delphinids, air is released from the lower airways through the tubular larynx into the bony narial spaces of the skull. This air is pressurized by piston-like actions of the larynx, and metered by the nasal plugs to the sound-producing phonic lips in the upper respiratory tract (Amundin and Andersen, 1983; Cranford et al., 2011). Therefore, the complex upper respiratory tract of odontocetes may represent an extension of dead space from the collapsing lower airways. A question, therefore, is to what degree vocalization or other 'shunting' of air into the upper airways may ultimately assist in voiding the lower airways of air in cetaceans. To continue vocalizing, the compressed small volume of air in the upper respiratory tract must be recycled (Amundin and Andersen, 1983; Dormer, 1979). Odontocetes have been noted to vocalize differently at increasing depth, indicating pressure-induced limitations of air management in the nasal passages. Sperm whales (*Physeter macrocephalus*) have been recorded to produce fewer clicks per block of click production at greater depth, indicating an apparent need for more frequent recycling of an increasingly small volume of compressed air (Wahlberg, 2002). *In situ* resonance spectrophotography of diving short-finned pilot whales (*Globicephala macrorhynchus*) has indicated that the amount of air needed per click, while remaining a very small volume (50 μl at 500 m, 100 μl at 1000 m), may vary depending on depth (Foskolos et al., 2019). Tonal sounds produced by delphinids, while more pneumatically expensive than clicks, can be produced at depth with unaffected frequency but decreased duration and output (Jensen et al., 2011). Therefore, key components of odontocete nasal anatomy as well as the lower airways are subject to pressure-induced functional changes, and additional studies may further clarify the usage of air within the cranial portion of the upper airway. The cetacean trachea must remain open under diving pressures to permit the passage of air into the upper respiratory tract from the lower airways. Study of the excised delphinid trachea has indicated an increased degree of stiffness that may assist in the maintenance of an open pathway (Bagnoli et al., 2011; Cozzi et al., 2005). A variety of anatomical and physiological aspects may enhance these properties in the living animal.

The gross morphology of the cetacean trachea is markedly different from that of terrestrial mammals as a result of the presence of spiraling tracheal rings without m. trachealis (Fig. 1A) (Cozzi et al., 2005). Furthermore, the cetacean trachea is distinguished from that of other marine mammals by the presence of the prominent submucosal lacunae, large venous spaces of vascularization (Fig. 1A) (Cozzi et al., 2005). It has been hypothesized that engorgement of these lacunae with blood may result in expansion of the luminal wall inwards, resulting in a narrower lumen and thicker tracheal walls. This flexible, expandable character of the cetacean trachea could further assist in maintaining an open airway during diving events (Ballarin et al., 2018). While this mechanism would effectively reduce the volume of the tracheal lumen, it could maintain an open path for air to void collapsing bronchial structures.

This study indicates that the cetacean bronchial structure exhibits greater compliance in comparison to the hypothesized stiff tracheal structure. Both cetacean species examined in this study exhibited visibly compliant bronchi, with those of the common dolphin being more compliant than those of the harbor porpoise. The larger bronchial volumes at the fullest inflations in comparison to half inflations at surface pressures for both cetaceans, as well as the common dolphin's variable collapse dynamics between inflation treatments suggest that diving lung volume plays a key role in maintaining maximum airway volume. It is worth noting that compliance studies of excised cetacean tracheas have revealed that common dolphin tracheas are more compliant during deflation than inflation, while the opposite is true of harbor porpoises (Moore et al., 2014). A reason for the apparent decreased compliance of the harbor porpoise airways may be related to the degree of inflation; if the calculated TLC_{ex} more closely relates to the TLC of a living animal, the harbor porpoise's fullest inflations were closer to this than those of the common dolphin (Table 2). However, the dynamics of the fullest inflation treatments of the common dolphin are still markedly different from both the fullest and half inflations of the harbor porpoise. Even if we assume that the calculated TLC_{ex}

is correct, and the 100% TLC_{tt} inflation treatments of the common dolphin and harbor porpoise were respectively closer to half and full TLC values of the living animals, we can then compare the 100% TLC_{tt} common dolphin and 50% TLC_{tt} harbor porpoise treatments with relevance. The common dolphin is still remarkable for its increased airway compliance and near-complete collapse at the highest pressures. Because of the small sample size, it is difficult to infer whether the observed differential in bronchial compliance between the two species represents a parallel species-specific difference, but it is worthwhile to consider the physiological consequences of such potential specialization. The harbor porpoise is a shallow diving cetacean, with average dive depths not exceeding 30 m (Linnenschmidt et al., 2013). The common dolphin, in contrast, is a moderately deep diver to average depths of over 60 m, with one recorded depth reaching 257 m (Evans, 1971). The more compliant bronchi in the common dolphin would initially appear to be a liability for its deeper diving behavior, because of the potentially slower voiding of air from the alveoli. It is worth considering, however, what function these compliant bronchi may fulfill once the air is voided from the alveoli. In the common dolphin with a diving lung volume equal to the measured TLC_{tt} (3000 ml), a pressure equivalent to 50 m resulted in an equivalent percentage decrease in volume in comparison to that for the harbor porpoise. In the common dolphin diving at half the measured TLC_{tt} (1500 ml), a pressure equivalent of a dive depth of 50 m resulted in a proportionally greater reduction of bronchial volume. This consisted primarily of complete flattening of the caudal aspects of the bronchi, while the tracheal bifurcation and a portion of the cranial primary bronchi remained partially open.

The question is raised whether a caudal to cranial collapse pattern represents an air-dependent hierarchy of compliance within the primary bronchi which effectively 'locks' air away from the smaller airways. This would ultimately channel air from the bronchi into the trachea and upper airways. The collapse of the lungs and bronchi therefore might be categorized as occurring in stages, with the first consisting of voiding of air from the alveoli into the compliant bronchi, which compress but remain open depending on the amount of air present. The contraction of myoelastic sphincters or comparable structures within the terminal bronchioles of many odontocetes could possibly further assist in preventing backflow of air into regions of gas exchange at this stage (Costa, 2007; Piscitelli et al., 2013). The next stage would represent voiding of air from the bronchi themselves through an ordered caudal to cranial collapse. The complete collapse of common dolphin bronchial volume to nearly 0 ml in both full and half lung volume treatments represents an almost complete isolation of the lungs and bronchi from air. The compliant bronchi in the common dolphin, while risking initial delay of air voiding, may actually represent an advantage for deeper diving as a result of a calibrated collapse response dependent on the total air volume voiding the lungs. This may result in the formation of a lock preventing backflow of pressurized air towards the surfaces of gas exchange and channeling air upwards into the short trachea and upper airways, where it may be used for sound production at depth. Historically, a variety of contrasting hypothesized functions related to air backflow and management have been assigned to the myoelastic sphincters, ranging from controlled alveolar air sequestration to prevention of backflow towards the alveoli (Costa, 2007; Fiebiger, 1916; Pabst et al., 1999; Piscitelli et al., 2013; Wislocki, 1929).

The adaptive significance of a short cervical length in obligate aquatic mammals has generally been attributed to the need for greater cervical stability while swimming, which is conducive to hydrodynamic form (Buchholtz, 2001). It could be speculated on the basis of our observations, however, that the reduced cervical and hence tracheal length of odontocetes also represents a fine-tuned adaptation for efficient movement of dive-compressed pulmonary air in the upper respiratory tract for echolocation. Assessment of a wide range of mammals has indicated that trachea length is roughly proportional to body mass[0.27] (Tenney and Bartlett, 1967), but a range of aquatic mammals have not been similarly assessed in this manner. Further studies comparing tracheal length in echolocating and non-echolocating obligate aquatic mammals may lend further insight into this question.

In contrast to odontocete cetaceans, pinnipeds are not known to employ sound production underwater for echolocation, although submerged vocalizations have been recorded for various species (Schevill et al., 1963). This indicates a difference in air management between cetaceans and pinnipeds, with less need for shunting of air within the upper airways of pinnipeds. Pinniped tracheal structure is not only longer but also notably more diverse in species-specific morphology when compared with that of cetaceans. In some species, this consists of varying tracheal ring morphology throughout the range of the tracheal length. For example, harbor seal tracheal structure consists of complete cartilaginous rings cranially, discontinuous rings with overlapping edges ('slip') and a gap filled with soft tissue in the midsection, and rings with a slip only caudally (Fig. 1B) (Moore et al., 2014). Similarly, gray seal tracheas are composed of complete tracheal rings in the cranial section, and discontinuous tracheal rings with a slip in the middle and caudal sections. In contrast to these two species, the harp seal trachea features discontinuous tracheal rings with a slip throughout its entire length (Moore et al., 2014). Ross seals (*Ommatophoca rossi*), northern elephant seals and Weddell seals have highly incomplete or horseshoe-shaped tracheal rings resulting in a comparatively flattened and compliant tracheal lumen (Kooyman and Andersen, 1969; Moore et al., 2014). Pinniped tracheal compliance may therefore vary depending on the region of the trachea as well as the species. In gray and harbor seals, the excised trachea consists of a less compliant cranial section and a more compliant caudal section, while the harp seal trachea is relatively compliant throughout its length (Moore et al., 2014). Therefore, the measured caudal tracheal samples of this study represent the more compliant portions of the trachea in the gray and harbor seals.

The pinniped airway measurements in this study provide the advantage of comparing bronchial measurements with those of tracheal segments from the same specimen. It is worth noting the relatively shallow percentage decrease in tracheal volume compared with bronchial volume in the gray and harbor seals. The 0–50 m treatments of both may indicate that the tracheal segments are less compliant than the bronchial sections. This indication is contradicted by the harp seal tracheal segment, which demonstrated a steep percentage decrease ultimately greater than that of the left bronchus. Regardless of any compliance differential between trachea and bronchi, all tracheal segments demonstrated measurable decreases in volume. In similar form to the bronchi of the common dolphin, this may represent a hierarchy of compliance which directs the air cranially. Alveolar collapse would lead to air entering the bronchi, which would ultimately channel to the trachea. The trachea, while not necessarily forming a complete lock, would collapse in whole or in part at its caudal extent, encouraging the air to flow towards the head. Caudal to cranial collapse patterns of this kind may require only minor differences in compliance between the components; Denison and Kooyman (1973) calculated that

the airways theoretically require compliance only five times that of the alveoli to facilitate efficient alveolar collapse. These changes represent isolation of air as far away from the regions of gas exchange as possible and further protection from backflow at depth. In the case of Ross and Weddell seals, which are known for prominent seasonal calls (Thomas and Kuechle, 1982; Watkins and Ray, 1985), this cranially sequestered air also may represent a critical functional component of submerged vocalization.

Of the pinnipeds, the harbor seal was the only species that exhibited near-complete collapse of both the tracheal and the bronchial sections at the maximum depth simulation (ca. 100 m.) Harbor seals may dive to mean depths of 12–40 m (Moore et al., 2009), and gray seals dive to mean depths of 48–51 m (Beck et al., 2000; Moore et al., 2009); on average, they are relatively shallow divers. Occasional very deep dives exceeding 400 m have been recorded for harbor seals (Eguchi and Harvey, 2005). Harp seals demonstrate mean diving depths of 89–106 m (Folkow et al., 2004; Lydersen and Kovacs, 1993), indicating somewhat deeper average diving abilities than those of harbor or gray seals. As the gray seal was pressurized to a simulated maximum depth of ca. 50 m, it is unfortunately impossible to make direct comparisons between the maximum depth compression dynamics of the gray and harbor seals. Furthermore, the harp seal represents the only full inflation pinniped treatment according to the measured TLC_{tt}, which raises the question of whether the maintenance of open airways at the maximum depth simulation (ca. 100 m) was due to the compliance characteristics of the airways or merely due to the larger amount of air in the airways. Interestingly, very deep diving pinniped species such as the Northern elephant seal, Ross seal and Weddell seal also have a highly compliant tracheal structure, the exact opposite of the stiffer airway structure of deep diving cetaceans (Kooyman and Andersen, 1969; Moore et al., 2014). Future studies may assist in further resolution of the function of these differentials in airway compliance observed between deep and shallow diving marine mammals.

This study represents the first volume quantified study of the bronchi of cetaceans and trachea and bronchi of pinnipeds under simulated diving pressures. All of the airways, far from behaving as perfectly rigid pipes, respond to pressure as compliant tubes to varying degrees. This study also demonstrates the ability of airways to return to an open luminal position, and the potential role of airway air content in compression dynamics. Taken as a whole, these findings from cadavers support previous studies indicating that a living marine mammal, whether a pinniped or cetacean, experiences a certain degree of tracheobronchial collapse during diving. The consequent delayed voiding of air from the lungs will result in alveolar collapse at deeper depths than that expected with rigid airway models. The theoretical physiological consequence would be an increased movement of pressurized gas into the bloodstream and vital organs under higher pressure (Kooyman et al., 1972; Moore et al., 2011). This would increase the likelihood of N_2 gas bubble emboli formation upon decompression, which is directly associated with the pathophysiology of decompression sickness (Fahlman, 2017; Francis and Mitchell, 2004).

Throughout mammalian physiology research, Scholander's concept of the shunt via compression has been the centrally held tenet of marine mammal avoidance of gas emboli formation and decompression sickness. However, development of a complete shunt may not be the only mechanism that prevents the pressurized N_2 gas exchange responsible for decompression sickness. It has been suggested that a selective control of cardiac output and lung perfusion may result in a ventilation–perfusion mis-match favorable

to O_2 and CO_2 exchange, but not N_2 (Garcia Párraga et al., 2018). Such a physiological mechanism, if verified, would greatly reduce the importance of rapid lung collapse and complete shunt formation in the avoidance of decompression sickness. Further studies related to this work would include full-length seal tracheal measurements under pressure and cetacean tracheal measurements. The use of live animals in similar studies is wrought with many possible ethical and logistical challenges, but if such studies could be ethically accomplished, they would represent a significant step forward in our understanding of respiratory physiology at depth.

Author contributions
Conceptualization: M.D., A.F.; Methodology: M.D., A.F., S.D.-G., M.M.; Software: M.D., S.D.-G., Z.S.; Validation: Z.S.; Formal analysis: M.D., S.D.-G., M.M.; Investigation: M.D., A.F., M.M.; Data curation: M.D., A.F., M.M.; Writing - original draft: M.D.; Writing - review & editing: M.D., A.F., S.D.-G., Z.S., M.M.; Supervision: A.F., S.D.-G., M.M.; Funding acquisition: M.M.

References
Amundin, M. and Andersen, S. H. (1983). Bony nares air pressure and nasal plug muscle activity during click production in the harbour porpoise, *Phocoena phocoena*, and the bottlenosed dolphin, *Tursiops truncatus*. *J. Exp. Biol.* **105**, 275-282.

Bagnoli, P., Cozzi, B., Zaffora, A., Acocella, F., Fumero, R. and Costantino, M. L. (2011). Experimantal and computational biomechanical characterisation of the tracheo-bronchial tree of the bottlenose dolphin (*Tursiops truncatus*) during diving. *J. Biomech.* **44**, 1040-1045. doi:10.1016/j.jbiomech.2011.02.005

Ballarin, C., Bagnoli, P., Peruffo, A. and Cozzi, B. (2018). Vascularization of the trachea in the bottlenose dolphin: comparison with bovine and evidence for evolutionary adaptations to diving. *R. Soc. open sci.* **5**, 171645. doi:10.1098/rsos.171645

Beck, C. A., Bowen, W. D. and Iverson, S. J. (2000). Seasonal changes in buoyancy and diving behaviour of adult grey seals. *J. Exp. Biol.* **203**, 2323-2330.

Bernaldo de Quirós, Y., Hartwick, M., Rotstein, D. S., Garner, M. M., Bogomolni, A., Greer, W., Niemeyer, M. E., Early, G., Wenzel, F. and Moore, M. (2018). Discrimination between bycatch and other causes of cetacean and pinniped stranding. *Dis. Aquat. Org.* **127**, 83-95. doi:10.3354/dao03189

Bostrom, B. L., Fahlman, A. and Jones, D. R. (2008). Tracheal compression delays alveolar collapse during deep diving in marine mammals. *Respir. Physiol. Neurobiol.* **161**, 298-305. doi:10.1016/j.resp.2008.03.003

Buchholtz, E. A. (2001). Vertebral osteology and swimming style in living and fossil whales (Order: Cetacea). *J. Zool.* **253**, 175-190. doi:10.1017/S0952836901000164

Costa, D. P. (2007). Diving physiology of marine vertebrates. In *Encyclopedia of Life Sciences* (ed. R. Baxter), pp. 1-7. John Wiley & Sons, Ltd.

Cozzi, B., Bagnoli, P., Acocella, F. and Constantino, M. L. (2005). Structure and biomechanical properties of the trachea of the striped dolphin *Stenella coeruleoalba*: evidence for evolutionary adaptations to diving. *Anat. Rec. A* **284A**, 500-510. doi:10.1002/ar.a.20182

Cranford, T. W., Elsberry, W. R., Van Bonn, W. G., Jeffress, J. A., Chaplin, M. S., Blackwood, D. J., Carder, D. A., Kamolnick, T., Todd, M. A. and Ridgway, S. H. (2011). Observation and analysis of sonar signal generation in the bottlenose dolphin (Tursiops truncatus): evidence for two sonar sources. *J. Exp. Mar. Biol. Ecol.* **407**, 81-96. doi:10.1016/j.jembe.2011.07.010

Denison, D. M. and Kooyman, G. L. (1973). The structure and function of the small airways in pinniped and sea otter lungs. *Respir. Physiol.* **17**, 1-10. doi:10.1016/0034-5687(73)90105-9

Dormer, K. J. (1979). Mechanism of sound production and air recycling in delphinids: cineradiographic evidence. *J. Acoust. Soc. Am.* **65**, 229-239. doi:10.1121/1.382240

Eguchi, T. and Harvey, J. T. (2005). Diving behavior of the Pacific harbor seal (*Phoca vitulina richardii*) in Monterey bay, California. *Mar. Mamm. Sci.* **21**, 283-295. doi:10.1111/j.1748-7692.2005.tb01228.x

Evans, W. E. (1971). Orientation behavior of delphinids: radio telemetric studies. *Ann. N. Y. Acad. Sci.* **188**, 142-160. doi:10.1111/j.1749-6632.1971.tb13094.x

Fahlman, A. (2017). Allometric scaling of decompression sickness risk in terrestrial mammals; cardiac output explains risk of decompression sickness. *Sci. Rep.* **7**, 40918. doi:10.1038/srep40918

Fahlman, A., Hooker, S. K., Olszowka, A., Bostrom, B. L. and Jones, D. R. (2009). Estimating the effect of lung collapse and pulmonary shunt on gas exchange during breath-hold diving: the Scholander and Kooyman legacy. *Respir. Physiol. Neurobiol.* **165**, 28-39. doi:10.1016/j.resp.2008.09.013

Fahlman, A., Loring, S. H., Ferrigno, M., Moore, C., Early, G., Niemeyer, M., Lentell, B., Wenzel, F., Joy, R. and Moore, M. J. (2011). Static inflation and deflation pressure-volume curves from excised lungs of marine mammals. *J. Exp. Biol.* **214**, 3822-3828. doi:10.1242/jeb.056366

Fahlman, A., Jensen, F., Tyack, P. L. and Wells, R. (2018). Modeling tissue and blood gas kinetics in coastal and offshore common Bottlenose dolphins, *Tursiops truncatus. Front. Physiol.* **9**, 838. doi:10.3389/fphys.2018.00838

Falke, K. J., Busch, T., Hoffmann, O., Liggins, G. C., Liggins, J., Mohnhaupt, R., Roberts, J. D., , Jr, Stanek, K. and Zapol, W. M. (2008). Breathing pattern, CO2 elimination and the absence of exhaled NO in freely diving Weddell seals. *Respir. Physiol. Neurobiol.* **162**, 85-92. doi:10.1016/j.resp.2008.04.007

Fiebiger, J. (1916). Über eigentümlichkeiten im aufbau der delphinlunge und ihre physiologische bedeutung. *Anat. Anz.* **48**, 540-565.

Fitzgerald, E. R. (1975). Dynamic mechanical measurements during the life to death transition in animal tissues. *Biorheology* **12**, 397-408. doi:10.3233/BIR-1975-12611

Folkow, L. P., Nordøy, E. S. and Blix, A. S. (2004). Distribution and diving behaviour of harp seals (*Pagophilus groenlandicus*) from the Greenland sea stock. *Polar Biol.* **27**, 281-298. doi:10.1007/s00300-004-0591-7

Foskolos, I., Aguilar de Soto, N., Madsen, P. T. and Johnson, M. (2019). Deep diving pilot whales make cheap, but powerful, echolocation clicks with 50 µl of air. *Sci. Rep.* **9**, 15720. doi:10.1038/s41598-019-51619-6

Francis, T. J. R. and Mitchell, S. J. (2004). Pathophysiology of decompression sickness. In *Bove and Davis' Diving Medicine* (ed. A. A. Bove), pp. 165-183. London, UK: Saunders, Elsevier Science Ltd.

Garcia Párraga, D., Moore, M. and Fahlman, A. (2018). Pulmonary ventilation–perfusion mismatch: a novel hypothesis for how diving vertebrates may avoid the bends. *Proc. R. Soc. B* **285**, 20180482. doi:10.1098/rspb.2018.0482

Hodanbosi, M. R., Sterba-Boatwright, B. and Fahlman, A. (2016). Updating a gas dynamics model using estimates for California sea lions (*Zalophus californianus*). *Respir. Physiol. Neurobiol.* **234**, 1-8. doi:10.1016/j.resp.2016.08.006

Hooker, S. K., Baird, R. W. and Fahlman, A. (2009). Could beaked whales get the bends? Effect of diving behaviour and physiology on modelled gas exchange for three species: ziphius cavirostris, mesoplodon densirostris and hyperoodon ampullatus. *Respir. Physiol. Neurobiol.* **167**, 235-246. doi:10.1016/j.resp.2009.04.023

Jensen, F. H., Perez, J. M., Johnson, M., Soto, N. A. and Madsen, P. T. (2011). Calling under pressure: short-finned pilot whales make social calls during deep foraging dives. *Proc. R. Soc. B* **278**, 3017-3025. doi:10.1098/rspb.2010.2604

Kida, M. Y. (1990). Morphology of the tracheobronchial tree of the Ganges river dolphin (*Platanista gangetica*). *Okajimas Folia Anat. Jpn.* **67**, 289-295. doi:10.2535/ofaj1936.67.4_289

Kooyman, G. L. (1973). Respiratory adaptations in marine mammals. *Am. Zool.* **13**, 457-468. doi:10.1093/icb/13.2.457

Kooyman, G. L. and Andersen, H. T. (1969). Deep diving. In *The Biology of Marine Mammals* (ed. H. T. Andersen), pp. 65-94. New York: Academic Press.

Kooyman, G. L. and Sinnett, E. E. (1982). Pulmonary shunts in harbor seals and sea lions during simulated dives to depth. *Physiol. Zool.* **55**, 105-111. doi:10.1086/physzool.55.1.30158447

Kooyman, G. L., Hammond, D. D. and Schroeder, J. P. (1970). Bronchograms and tracheograms of seals under pressure. *Science* **169**, 82-84. doi:10.1126/science.169.3940.82

Kooyman, G. L., Schroeder, J. P., Denison, D. M., Hammond, D. D., Wright, J. J. and Bergman, W. P. (1972). Blood nitrogen tensions of seals during simulated deep dives. *Am. J. Physiol.* **223**, 1016-1020. doi:10.1152/ajplegacy.1972.223.5.1016

Kooyman, G. L., Ponganis, P. J. and Howard, R. S. (1999). Chapter 14: Diving animals. In *"The Lung at Depth"* (ed. C. Lundgren and J. Miller), pp. 587-620. New York: Marcel Dekker.

Laakkonen, J. and Jernvall, J. (2016). Macroscopic anatomy of the Saimaa ringed seal (*Phoca hispida saimensis*) lower respiratory tract. *Anat. Rec.* **299**, 538-543. doi:10.1002/ar.23316

Leith, D. E. (1989). Adaptations to deep breath-hold diving: respiratory and circulatory mechanics. *Undersea Biomed. Res.* **16**, 345-354.

Leith, D. E., Lowe, R. and Gillespie, J. (1972). Mechanics of baleen whale lungs. *Fed. Proc.* **31**, 335.

Linnenschmidt, M., Teilmann, J., Akamatsu, T., Dietz, R. and Miller, L. A. (2013). Biosonar, dive, and foraging activity of satellite tracked harbor porpoises (Phocoena phocoena). *Mar. Mamm. Sci.* **29**, E77-E97. doi:10.1111/j.1748-7692.2012.00592.x

Lydersen, C. and Kovacs, K. M. (1993). Diving behaviour of lactating harp seal, Phoca groenlandica, females from the Gulf of St Lawrence, Canada. *Anim. Behav.* **46**, 1213-1221. doi:10.1006/anbe.1993.1312

McDonald, B. I. and Ponganis, P. J. (2012). Lung collapse in the diving sea lion: hold the nitrogen and save the oxygen. *Biol. Lett.* **8**, 1047-1049. doi:10.1098/rsbl.2012.0743

Moore, M. J., Bogomolni, A. L., Dennison, S. E., Early, G., Garner, M. M., Hayward, B. A., Lentell, B. J. and Rotstein, D. S. (2009). Gas bubbles in seals, dolphins, and porpoises entangled and drowned at depth in gillnets. *Vet. Pathol.* **46**, 536-547. doi:10.1354/vp.08-VP-0065-M-FL

Moore, M. J., Hammar, T., Arruda, J., Cramer, S., Dennison, S., Montie, E. and Fahlman, A. (2011). Hyperbaric computed tomographic measurement of lung compression in seals and dolphins. *J. Exp. Biol.* **214**, 2390-2397. doi:10.1242/jeb.055020

Moore, C., Moore, M., Trumble, S., Niemeyer, M., Lentell, B., McLellan, W., Costidis, A. and Fahlman, A. (2014). A comparative analysis of marine mammal tracheas. *J. Exp. Biol.* **217**, 1154-1166. doi:10.1242/jeb.093146

Nakakuki, S. (1994). The bronchial tree and lobular division of the lung in the striped dolphin (*Stenella coeruleo-albus*). *J. Vet. Med. Sci.* **56**, 1209-1211. doi:10.1292/jvms.56.1209

Pabst, D. A., Rommel, S. A. and McLellan, W. A. (1999). The functional morphology of marine mammals. In *Biology of Marine Mammals* (ed. J. E. Reynolds and S. A. Rommel), pp. 15-72. Washington: Smithsonian Institution Press.

Piscitelli, M. A., Raverty, S. A., Lillie, M. A. and Shadwick, R. E. (2013). A review of cetacean lung morphology and mechanics. *J. Morphol.* **274**, 1425-1440. doi:10.1002/jmor.20192

Ridgway, S. H. and Howard, R. (1979). Dolphin lung collapse and intramuscular circulation during free diving: evidence from nitrogen washout. *Science* **206**, 1182-1183. doi:10.1126/science.505001

Ridgway, S. H., Scronce, B. L. and Kanwisher, J. (1969). Respiration and deep diving in the bottlenose porpoise. *Science* **166**, 1651-1654. doi:10.1126/science.166.3913.1651

Schevill, W. E., Watkins, W. A. and Ray, C. (1963). Underwater sounds of pinnipeds. *Science* **141**, 50-53. doi:10.1126/science.141.3575.50

Scholander, P. F. (1940). Experimental investigations on the respiratory function in diving mammals and birds. *Hvalrådets Skr.* **22**, 1-131.

Smith, E. C. B. (1939). Changes in elasticity of mammalian muscle undergoing rigor mortis. *J. Physiol.* **96**, 176-193. doi:10.1113/jphysiol.1939.sp003769

Stephenson, R. (2005). Physiological control of diving behaviour in the Weddell seal Leptonychotes weddelli: a model based on cardiorespiratory control theory. *J. Exp. Biol.* **208**, 1971-1991. doi:10.1242/jeb.01583

Tarasoff, F. J. and Kooyman, G. L. (1973). Observations on the anatomy of the respiratory system of the river otter, sea otter, and harp seal. II. The trachea and bronchial tree. *Can. J. Zool.* **51**, 171-177. doi:10.1139/z73-025

Tenney, S. M. and Bartlett, D. (1967). Comparative quantitative morphology of the mammalian lung: trachea. *Respir. Physiol.* **3**, 130-135. doi:10.1016/0034-5687(67)90002-3

Thomas, J. A. and Kuechle, V. B. (1982). Quantitative analysis of Weddell seal (*Leptonychotes weddelli*) underwater vocalizations at McMurdo Sound, Antarctica. *J. Acoust. Soc. Am.* **72**, 1730-1738. doi:10.1121/1.388667

Tift, M. S., Hückstädt, L. A., McDonald, B. I., Thorson, P. H. and Ponganis, P. J. (2017). Flipper stroke rate and venous oxygen levels in free-ranging California sea lions. *J. Exp. Biol.* **220**, 1533-1540. doi:10.1242/jeb.152314

Wahlberg, M. (2002). The acoustic behaviour of diving sperm whales observed with a hydrophone array. *J. Exp. Mar. Biol. Ecol.* **281**, 53-62. doi:10.1016/S0022-0981(02)00411-2

Watkins, W. A. and Ray, G. C. (1985). In-air and underwater sounds of the Ross seal, Ommatophoca rossi. *J. Acoust. Soc. Am.* **77**, 1598-1600. doi:10.1121/1.392003

Wislocki, G. B. (1929). On the structure of the lungs of the porpoise (*Tursiops truncatus*). *Am. J. Anat.* **44**, 47-77. doi:10.1002/aja.1000440103